JOURNAL OF SCIENTIFIC RESEARCH IN ALLIED SCIENCES
ISSN NO. 2455-5800
Contents available at www.jusres.com

INTEGRATED GEOPHYSICAL AND GEOCHEMICAL APPROACH TO INVESTIGATE CONTAMINATION OF AQUIFER POTENTIAL IN ABANDONED DUMPSITE IN OGBOVWAN TOWN, UGHELLI-NORTH LOCAL GOVERNMENT AREA, DELTA STATE, NIGERIA

*Omamode Samuel Marere[1], Essono Emmanuel Allen[1]
1. Department of Science Laboratory Technology, Federal Polytechnic Orogun, 10 Orhomuru-Orogun Road, Orogun, Delta State, Nigeria.

ARTICLE INFO **ABSTRACT** **ORIGINAL RESEARCH ARTICLE**

Article History
Received: Oct. 2024
Accepted: Nov. 2024
Keywords: leachate, dumpsite, geophysical, aquifer, dipole-dipole

Corresponding Author
*O. S. Marere

This study utilizes an integrated geophysical and geochemical approach to evaluate groundwater contamination in aquifers located beneath an abandoned dumpsite in Ogbovwan Town, Delta State, Nigeria. The main goal is to assess the degree of leachate penetration into the aquifer system and its impact on water quality. Geophysical methods, such as Electrical Resistivity Tomography (ERT) and Vertical Electrical Sounding (VES), are combined with geochemical analysis of groundwater samples to comprehensively understand the subsurface conditions and contamination levels. The analysis shows that the mean pH concentration of the groundwater is 4.625, which is below the recommended WHO (2011) and NSDWQ (2007) standards of 6.5-8.5, indicating that the groundwater is acidic. This acidity can significantly impact water quality by increasing the solubility and mobility of metals. Additionally, the mean levels of lead (Pb) and cadmium (Cd) are found to be 0.013 mg/L, exceeding the permissible limits set by WHO and NSDWQ, highlighting the presence of contaminants in the groundwater, making it unsafe for drinking. Geophysical survey results further identify low-resistivity zones beneath the dumpsite, suggesting leachate infiltration into the subsurface layers. This finding confirms that contaminants from the dumpsite are migrating into the aquifer, impacting the groundwater quality within the research location.

1. INTRODUCTION

The environment exhibits an important role in human existence, as it provides foundation for habitation and sustains life. A dumpsite is a designated area for disposing of waste products, such as domestic trash, building debris, and industrial waste. Dumpsites can be classified as either formal, regulated sites managed by local authorities, or informal, unregulated areas where waste accumulates. Unlike modern landfills, which are engineered to minimize environmental impact, dumpsites often lack proper management, resulting in issues such as pollution, groundwater contamination, and health hazards for nearby communities. An abandoned dumpsite refers to a location where waste was once disposed of but has since been left unmanaged and neglected. Although these sites are no longer used for waste disposal, the accumulated waste remains, leading to significant environmental and health risks over

time. These risks include the release of harmful gases, soil and water contamination, and the potential spread of diseases. Without appropriate rehabilitation or cleanup efforts, abandoned dumpsites can continue to degrade the surrounding environment and adversely affect nearby communities. Such sites are critical sources of environmental pollution, particularly concerning groundwater contamination. Leachates from decomposing organic and inorganic materials can migrate through the soil and infiltrate aquifers, posing serious risks to public health. This research focuses on assessing the potential for aquifer contamination at the abandoned dumpsite in Ogbovwan Town, where improper waste disposal practices have raised significant concerns about groundwater quality. Water pollution disrupts the natural balance of water bodies due to both natural and human activities, negatively impacting aquatic organisms and the overall environment [1] [2]. Emphasizing cost-effective geophysical surveys is essential for accurately identifying plumes, estimating quantities, and delineating areas of contaminants in groundwater. The proof of groundwater contamination can be achieved through the monitoring of well networks tailored based on the plumes and subsurface stratigraphy defined by these geographical surveys [3].

The natural vulnerability of an aquifer refers to its susceptibility to negative effects from an applied pollution load. Groundwater becomes contaminated when pollutants are released into the ground which eventually percolate into the groundwater supply [4]. Water pollution results mainly from 'point' sources and 'diffuse' sources. Point sources are locations from which pollutants are discharged, such as domestic sewage, industrial effluents, and livestock wastewater. Pollution from point sources can be minimized by centrally collecting, treating, and potentially recycling these wastes to acceptable levels for various beneficial uses. In contrast, diffuse sources are those whose specific locations are not easily identifiable. Water pollution resulting from diffuse sources, such as agricultural runoff, can be managed by altering cropping patterns, improving tillage practices, and implementing advanced farm management techniques that reduce contamination of water bodies [5].

1.1 Review of Study Location

Ogbovwan is a town located in Delta State, Nigeria, and experiences high levels of precipitation, increasing the risk of leachate migration into the underlying aquifers. The abandoned dumpsite, once used for waste disposal, has been left unmanaged, leading to concerns about contamination of the surrounding environment, including groundwater sources that serve local communities. The dumpsite was in use from 2014 to 2021. The dumpsite is municipal domestic dumpsite as shown in Plate 1. The people in the study area are majorly crop and livestock farmers. Figure 1 show the sampling points where groundwater samples was collected and where geophysical survey was carryout around the study area as shown in Plate 1 and the coordinate point are shown in Table 1.

Plate 1: A view of the abandoned waste dumpsite

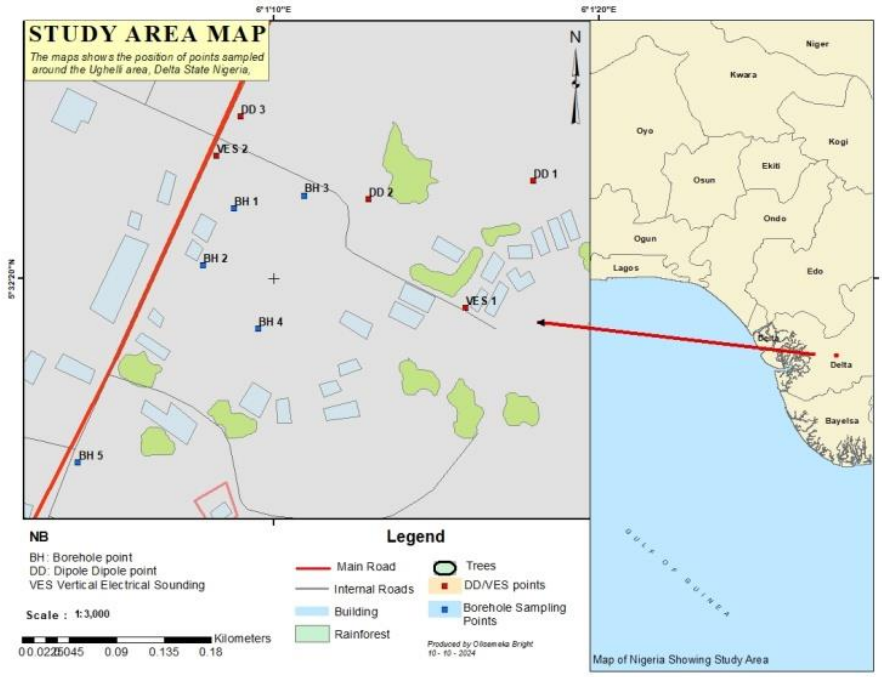

Figure 1: Map of the study area

1.2 Geology of the Study Area

The Delta Region is underlain by Sedimentary Formation of the South Sedimentary Basin, it consists of the Benin Formation, alluvial deposits, topsoil, and the Azagba Ogwashi (Asaba-Ogwashi) Formation. The geology which is characterized by the lateritized clay and sand features sandstone originating from PaleoCoastal environment of the Palaeocene-Pleistocene Age. These sediments extend across the southern fringes of the Anambra Basin, representing the upper facies off-flaps of the Niger Delta. Known as Coastal Plain sands, this formation consists of red earth underlain by sands and clays from an ancient Coastal Plain environment, now visible in Owerri, Calabar, Onitsha, and the Delta region, dated to the Oligocene-Pleistocene period [6]. The Benin formation dips southward in the study area, which is located within the Niger Delta Basin. The Sombreiro Deltaic features and Benin formation are characterized by sedimentary environments: marine, mixed and continental. Due to sedimentary environmental classification, there are three rock formations such as: Benin, Agbada, and Akata. In the Niger Delta oil-producing communities, the source and seal rocks are the marine/deltaic, plastic, and over-pressured shales of the Akata and Agbada formations [7]. The study area geologically includes clay, sand, pebbles, sandstone, gravel, shales, mangrove swamp, lignite, and alluvium. The aquifers of the Benin formation fulfill the regions groundwater needs. The poorly sorted coastal sands become sandier and more unconsolidated towards the surface. This increases porosity and permeability, and thereby the storage coefficient of the aquifer. Recharge from surrounding water bodies and heavy rainfall percolating through the dense vegetation is minimal, resulting in a highly productive hydrologic unit within the area.

Vertical electrical sounding (VES) is a resistivity technique employed for depth sounding because of its dependability and straightforwardness [9] and it is also utilized to access the vertical changes in apparent resistivity beneath the earth's surface [10]. Given that the apparent resistivity of most rocks depends on the volume of water in the pore spaces within them [11]. The objective of this research is to determine the pollution plume movement and its impact on groundwater of the study area. Electrical method of geophysical survey was adopted; the arrays used are Dipole-Dipole and Schlumberger arrays.

2. MATERIALS AND METHODS

2.1 MATERIALS

In this research work, four (4) Groundwater samples and Control water sample was collected around the abandoned dumpsite and geophysical survey was also carried out as shown in Figure 1. Parameters such as pH, electrical conductivity, Total Dissolved Solids (TDS), Calcium, Potassium, Sodium, nitrate, carbonate, chloride, Sulphate, Magnesium, heavy metals (manganese, iron, Copper, Zinc, Lead, Cadmium, Chromium, Nickel and Cobalt), and organic contaminants are analyzed to evaluate the level of contamination. Geophysical survey was conducted at old dumpsite in Esefieta layout of Ogbovwan Community, Delta State. The survey took two days from 22nd to 23rd August, 2024. The electrical resistivity tomography (ERT) and vertical electrical sounding (VES) techniques are used to map the subsurface lithology and detect zones of potential leachate plumes. The resistivity profiles help identify contaminated zones with high conductivity due to leachate intrusion of the study area. The water samples were to the laboratory for physiochemical and heavy metals parameter. The Dipole-Dipole and Schlumberger array of Electrical Resistivity Survey method was adopted. Petrozenith Terrameter was used to carry out this survey which is powered by a 12.5v D.C power source. According to [12], other accessories connected to the Terrameter include a booster, four metal electrodes, cables for the current and potential electrodes, three hammers, measuring tapes, and mobile phones for facilitating long-distance communication as shown in Plate 2. The Dipole-Dipole array, also referred to as 2D resistivity surveying, utilizes an electrode spacing configuration of 10 meters. The coordinate points and sampling points are shown in Table 1.

Plate 2: Equipment setups along Ofuoma express way

Table 1: Coordinate points and Sampling points

Borehole Water Samples	
Sampling points	Coordinate points
BH 1	N5°32´22.17" E6°1´8.8"
BH 2	N5°32´20.41" E6°1´7.84"
BH 3	N5°32´22.56" E6°1´10.96"
BH 4	N5°32´18.46" E6°1´9.55"
BH 5	N5°32´14.34" E6°1´4.00"
Geophysical Survey Points (Dipole-Dipole DD) and (VES)	
DD 1	N5°32´23" E6°1´18"
DD 1	N5°32´22.452" E6°1´12.936"
DD 1	N5°32´25" E6°1´9"
VES 1	N5°32´19.086" E6°1´15.918"
VES 2	N5°32´23.79" E6°1´8.26"

2.2 METHODS

2.2.1 DIPOLE-DIPOLE ARRAY

Dipole-Dipole array uses superficial resistivity to form 2D imaging which stands as different layers in subsurface soil. The difference between the current electrode pair, C2-C1, is denoted as 'a' [11] [12], which is equal to the space between the potential electrode pair, P1-P2. The array has another factor marked as 'n' which is the ratio between the C1 and P1 electrodes to C2-C1 (or P1-P2) dipole separation 'a'. For surveys using this array, the 'a' spacing is initially maintained as constant while the 'n' factor is increased incrementally from 1 to 2, 3, and up to approximately 6 in order to extend the depth of investigation [13]. The array is highly sensitive to resistivity changes between the electrodes in each dipole pair, with the sensitivity contour pattern being nearly vertical. This makes the dipole array particularly sensitive to horizontal changes in resistivity [14] That means it is good in mapping vertical structures, such as dykes and cavities, but relatively poor in mapping horizontal structures such as sills or sedimentary layers [15]. The median depth of investigation of this array also depends on the 'n' factor, as well as 'a' factor.

The formular for Geometric factor (G) and Apparent resistivity (ρa) for Dipole-Dipole array is given as:

$$G = \pi na((n+1)(n+2)) \text{ -----Equation 1}$$

2.2.2 SCHLUMBERGER ARRAY

The Schlumberger configuration was applied for vertical electrical sounding, with a maximum current electrode separation (AB) of 300m, which allowed a depth penetration of 150m (AB/2). The potential electrode spacing was increased several times during the sounding, from MN/2 equal to 0.5m to 6m. A Garmin GPS instrument was used to determine well coordinates and elevation of the study area. Different electrode spacings was utilized based on the part of the earth where anomalies are to be investigated[12]. The current electrodes C1 and C2 were projected outward symmetrically while maintaining the potential electrodes P1 and P2 at the center. Field-obtained VES data were manually plotted on a graph showing visible resistivity against half-

electrode spacing. Parameters like superficial resistivity and thickness, derived from the curve matching, were used as input data for computer iterative modelling [15].

The formula for geometric factor (G) and Superficial Resistivity (ρa) for Schlumberger array is given as:

$$Pa = K\frac{\Delta V}{I}$$ ----------Equation 2

2.2.3 DATA PROCESSING

The data gathered were pre-processed by ensuring data quality, and calculating the resistivity of the different readings by multiplying them with the necessary constant. Also, field graphs were plotted using manual graphs. The IX1Dv3 and Dipro software application was utilized to achieve the thickness and resistivity values. The Schlumberger values was first manually curve matched before inserting them into the computer software program to obtain the resistivity model parameters and the values is now run by the program as a routine which in turn displayed an automatically plotted graph with an error tolerance limit set forth eprogram. The data gotten from Schlumberger and Dipole-Dipole array were analyzed using the geophysical software IX1Dv3 and Dipro. The geoelectric layers, depth was generated, as well as the resistivity spread. The analyzed data was interpreted to determine the aquifer potential and delineate the lithology of the investigated area. When this iteration is done, the model parameters become the interpreted geoelectric layer [12].

3. RESULTS

PHYSIOCHEMICAL PARAMETERS OF WATER SAMPLES COLLECTED AROUND ABANDON DUMPSITE AT OGBOVWAN COMMUNITY

The pH concentration ranges from 4.5 to 4.9, with an average of 4.62. Total Dissolved Solids (TDS) range from 35 to 45 mg/L, with an average of 40 mg/L. Electrical Conductivity (EC) varies between 74 and 92 µS/cm, with an average of 82.5 µS/cm. Magnesium (Mg) concentrations range from 0.3 to 1.6 mg/L, averaging 0.95 mg/L. Calcium (Ca) ranges from 0.6 to 0.9 mg/L, with an average of 0.75 mg/L. Potassium (K) concentrations range from 0.3 to 1.6 mg/L, averaging 0.95 mg/L. Sodium (Na) ranges from 2.0 to 2.1 mg/L, with an average of 2.05 mg/L. Nitrate (NO_3^-) varies from 0.02 to 0.51 mg/L, with an average of 0.265 mg/L. Bicarbonate (HCO_3^-) ranges from 100 to 150 mg/L, with an average of 118.25 mg/L. Chloride (Cl^-) concentrations range from 0.3 to 0.8 mg/L, averaging 0.575 mg/L. Sulphate (SO_4^{2-}) varies from 0.24 to 0.49 mg/L, with an average of 0.307 mg/L, as detailed in Table 2, and Figures 1 and 2. The concentration values of these physiochemical parameters in the control water sample comply with NSWDQ (2007) and WHO (2011) standards, as shown in Table 2 and Figures 2, 3 and 4.

HEAVY METALS OF WATER SAMPLES COLLECTED AROUND ABANDON DUMPSITE AT OGBOVWAN COMMUNITY

The concentration of Manganese (Mn) ranges from 0.01 to 0.021 mg/L, with an average of 0.016 mg/L. Iron (Fe) ranges from 0.055 to 0.074 mg/L, with an average of 0.0625 mg/L. Copper (Cu) concentrations vary between 0.03 and 0.045 mg/L, averaging 0.038 mg/L. Zinc (Zn) ranges from 0.085 to 0.326 mg/L, with an average of 0.255 mg/L. Cobalt (Co) concentrations range from 0.009 to 0.013 mg/L, with an average of 0.007 mg/L. Nickel (Ni) ranges from 0.012 to 0.017 mg/L, with an average of 0.0145 mg/L. Chromium (Cr) concentrations range from 0.012 to 0.016 mg/L, with an average of 0.012 mg/L. Cadmium (Cd) ranges from 0.01 to 0.17 mg/L, with an average of 0.0132 mg/L. Lead (Pb) concentrations range from 0.011 to 0.015 mg/L, with an average of 0.013 mg/L. The concentration values of heavy metals in the control water sample range from 0.002 to 0.09 mg/L, with a standard deviation between 0.002 and 0.079, which is below the mean concentration of the study, as illustrated in Table 3 and 4, Figures 5 and 6.

Table 2: Physiochemical Parameters of water Samples Collected with NSWDQ (2007) and WHO Limit (2011)

S/N	Parameters	Loc. 1	Loc. 2	Loc. 3	Loc. 4	Mean Con.	Control	NSWDQ (2007)	WHO Limit 2011
1	Mg (mg/L)	0.4	0.3	1.5	1.6	0.95	0.1	50	100
2	Ca (mg/L)	0.8	0.6	0.7	0.9	0.75	0.2	75	200
3	K (mg/L)	2.1	2	2	2.1	2.05	0.7		
4	Na (mg/L)	9.7	9.5	10	10.2	9.85	5.19	200	200
5	NO_3^- (mg/L)	0.51	0.49	0.02	0.04	0.265	0.02	50	50
6	HCO_3^- (mg/L)	150	100	112	111	118.25	50.0		
7	Cl^- (mg/L)	0.7	0.3	0.5	0.8	0.575	0.1	250	250
8	SO_4^{2-} (mg/L)	0.28	0.24	0.46	0.49	0.3675	0.07	100	250
9	pH	4.9	4.4	4.3	4.9	4.625	7.00	6.5-8.5	6.5-8.5
10	TDS (mg/L)	45	40	35	38	39.5	25.1	500	1000
11	EC (µS/cm)	92	90	74	78	83.5	62.0	1000	900
	Mean Con.	27.853	22.53	21.862	22.548	23.698	13.68		

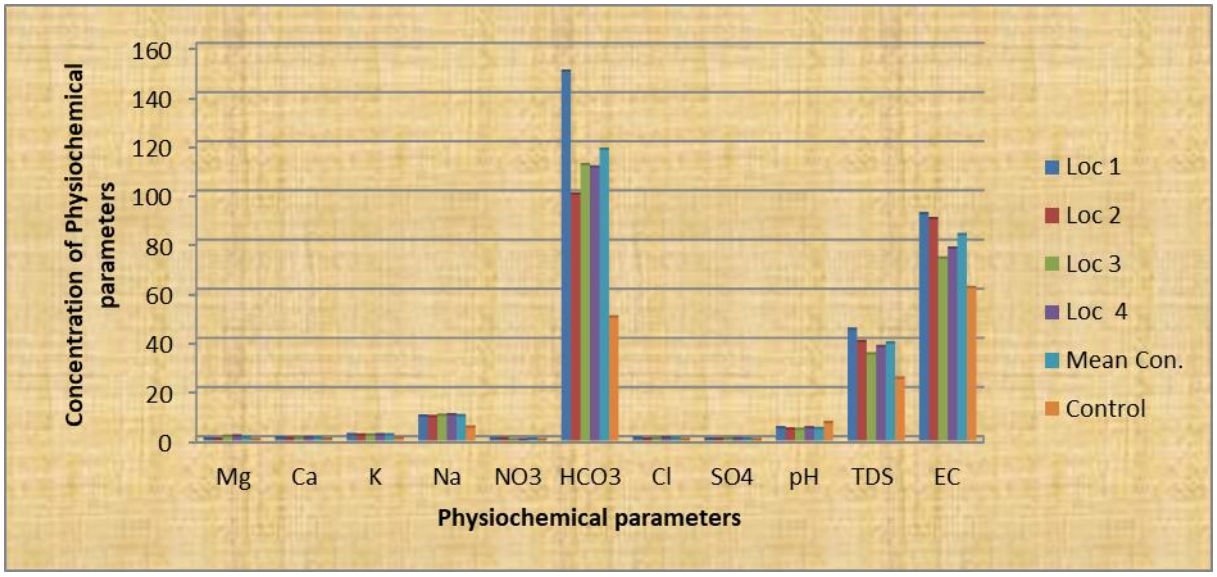

Figure 2: Concentration of physiochemical parameters with physiochemical parameters

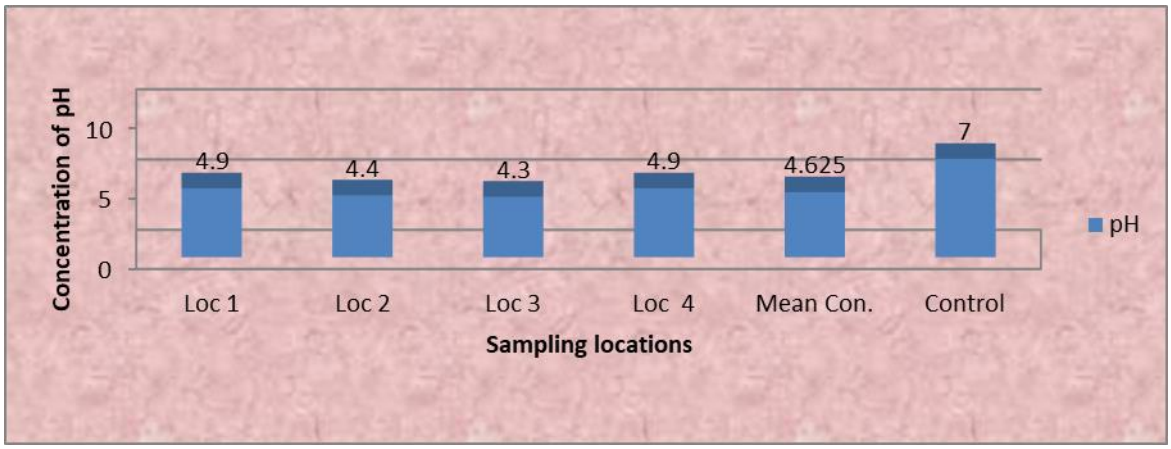

Figure 3: Concentration of pH against sampling locations

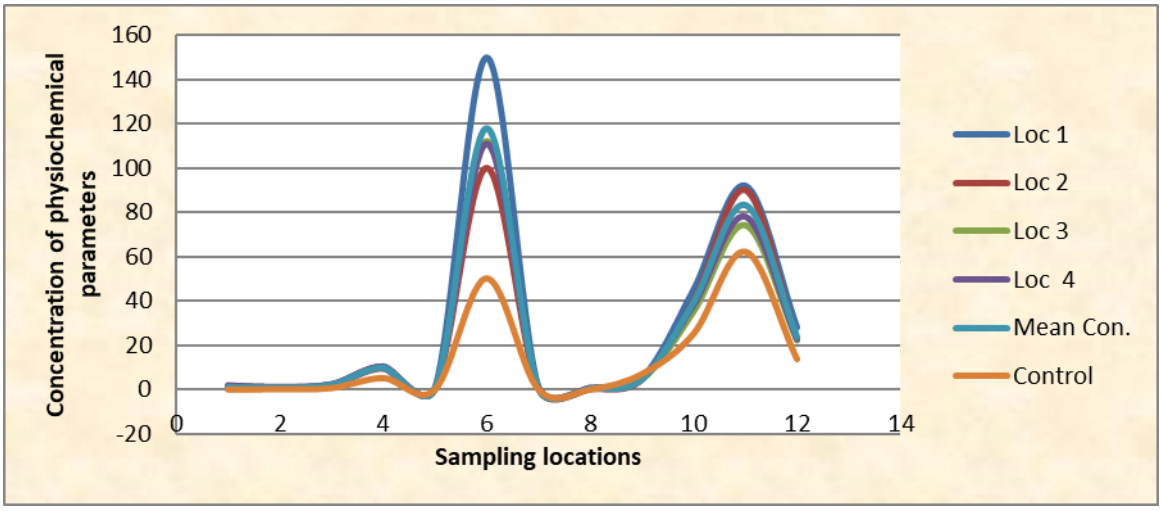

Figure 4: Scatter diagram of the concentration of physiochemical parameters and sampling locations

Table 3: Heavy metal parameters and statistical parameters of the study area

S/N	Parameters (mg/L)	Loc 1	Loc 2	Loc 3	Loc 4	Mean Con.	Control	Std. Dev.
1	Mn	0.020	0.019	0.01	0.013	0.016	0.008	0.005
2	Fe	0.074	0.07	0.05	0.056	0.062	0.006	0.011
3	Cu	0.045	0.042	0.03	0.038	0.039	0.01	0.006
4	Zn	0.326	0.321	0.185	0.189	0.255	0.09	0.079
5	Pb	0.015	0.013	0.011	0.014	0.013	0.004	0.002
6	Cr	0.016	0.013	0.015	0.012	0.014	0.003	0.002
7	Cd	0.01	0.017	0.012	0.014	0.013	0.002	0.003
8	Ni	0.017	0.014	0.012	0.015	0.014	0.004	0.002
9	Co	0.011	0.009	0.01	0.013	0.011	0.09	0.002

Table 4: Comparison of Heavy metal parameters with NSWDQ (2007) and WHO (2011) standard values

S/N	Parameters (mg/L)	Loc 1	Loc 2	Loc 3	Loc 4	Mean Con.	Control	NSWDQ (2007)	WHO Limit (2011)
1	Mn	0.020	0.019	0.01	0.013	0.016	0.008	0.2	0.4
2	Fe	0.074	0.07	0.05	0.056	0.0625	0.006	0.3	0.3
3	Cu	0.045	0.042	0.03	0.038	0.039	0.01	1	2.0
4	Zn	0.326	0.321	0.185	0.189	0.255	0.09	3	5.0
5	Pb	0.015	0.013	0.011	0.014	0.013	0.004	0.01	0.01
6	Cr	0.016	0.013	0.015	0.012	0.014	0.003	0.05	0.05
7	Cd	0.01	0.017	0.012	0.014	0.013	0.002	0.01	1.0
8	Ni	0.017	0.014	0.012	0.015	0.014	0.004	0.02	0.02
9	Co	0.011	0.009	0.01	0.013	0.011	0.09	0.05	1.0`
	Mean Con	0.059	0.057	0.037	0.040	0.049	0.024		

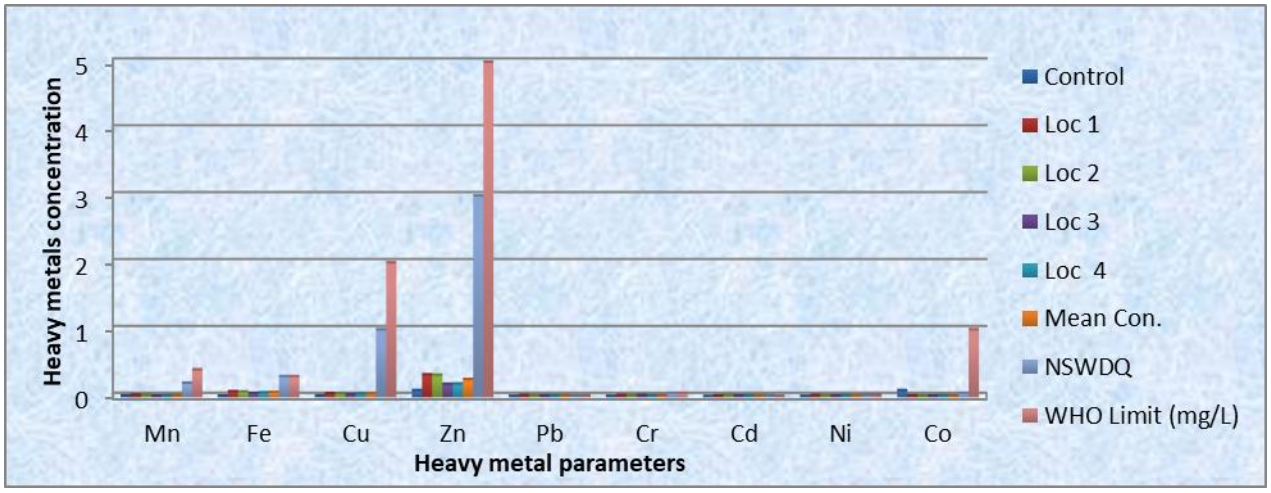

Figure 5: Concentration of Heavy metal parameters and Heavy metal parameters

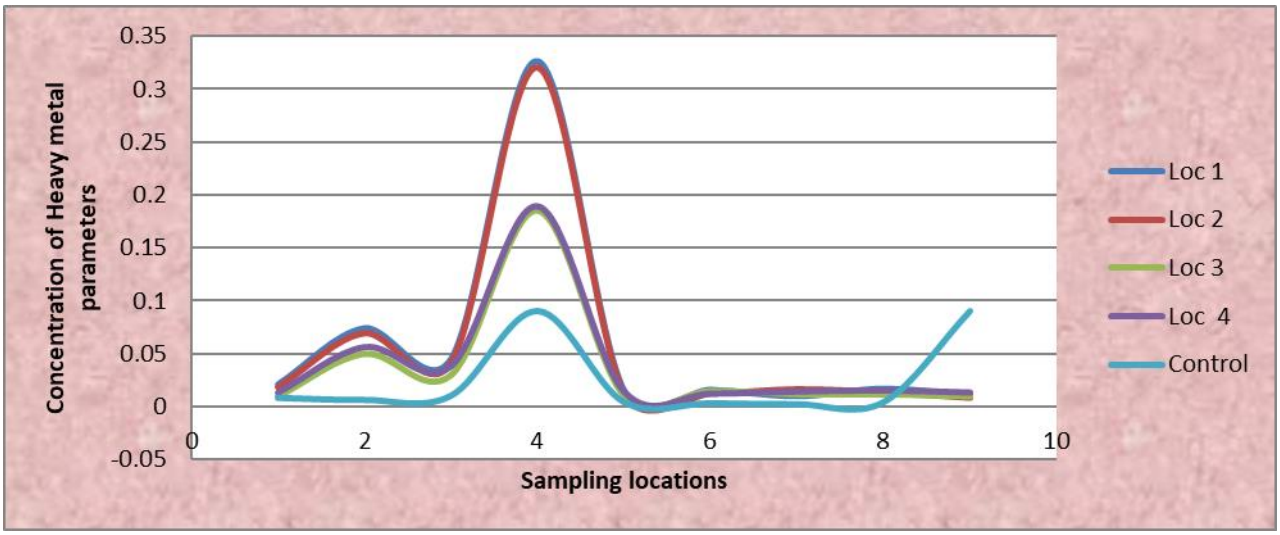

Figure 6: Scatter diagram of the concentration of Heavy metal parameters and sampling locations

Table 5: Field data of Dipole-Dipole 1 at Old Dumpsite in Esefieta Layout

RESISTIVITY FIELD RECORD							
Site Description: Old Dumpsite in Esefieta Layout, Ogbovwan Community, Delta State					Operation: Omamode Samuel Marere		
Equipment: Petrozenith Terrameter					Survey direction: SE Direction		
Date: 22/08/2024					Electrode Array: Dipole-Dipole 1		
Electrode Spacing: 10m					Elevation:		
Electrode position (m)				Geometric Factor	Resistance Ω	Superficial Resistivity Ωm	Coordinate of Stations
C1	C2	P1	P2				
0	10	20	30	188.52	2.02	380.8104	N5° 32′ 23″ E6° 1′ 8″
		30	40	754.08	3.02	2277.3216	
		40	50	1885.2	2.34	4411.368	
		50	60	3770.4	2.72	10255.488	
		60	70	6598.2	2.11	13922.202	
10	20	30	40	188.52	4.00	754.08	N5° 32′ 23″ E6° 1′ 8″
		40	50	754.08	2.25	1696.68	

		50	60	1885.2	2.06	3883.512	
		60	70	3770.4	2.55	9614.52	
		70	80	6598.2	0.6945	4582.4499	
20	30	40	50	188.52	0.7808	147.1964	N5° 32′ 23″ E6° 1′ 9″
		50	60	754.08	0.125	94.26	
		60	70	1885.2	0.5381	1014.4261	
		70	80	3770.4	0.6276	2366.3030	
		80	90	6598.2	3.35	22103.97	
30	40	50	60	188.52	0.4268	80.4603	N5° 32′ 23″ E6° 1′ 9″
		60	70	754.08	0.4227	318.7496	
		70	80	1885.2	2.04	3845.808	
		80	90	3770.4	0.938	3536.6352	
		90	100	6598.2	0.3397	2241.4085	
40	50	60	70	188.52	1.08	203.6016	N5° 32′ 23″ E6° 1′ 9″
		70	80	754.08	8.77	6613.2816	
		80	90	1885.2	12.49	23546.148	
		90	100	3770.4	2.47	9312.888	
		100	110	6598.2	0.6451	4256.4988	
50	60	70	80	188.52	2.03	382.6956	N5° 32′ 23″ E6° 1′ 10″
		80	90	754.08	0.713	537.6590	
		90	100	1885.2	3.62	6824.424	
		100	110	3770.4	1.05	3958.92	
		110	120	6598.2	0.138	910.5516	
60	70	80	90	188.52	0.624	117.6365	N5° 32′ 23″ E6° 1′ 10″
		90	100	754.08	0.307	231.5026	
		100	110	1885.2	0.41535	783.0178	
		110	120	3770.4	0.2786	1050.4334	
		120	130	6598.2	2.12	13988.184	
70	80	90	100	188.52	4.53	853.9956	N5° 32′ 23″ E6° 1′ 11″
		100	110	754.08	5.58	4207.7664	
		110	120	1885.2	5.31	10010.412	
		120	130	3770.4	0.203	765.3912	
		130	140	6598.2	0.182	1200.8724	
80	90	100	110	188.52	0.366	68.9983	N5° 32′ 23″ E6° 1′ 11″
		110	120	754.08	0.413	311.4350	
		120	130	1885.2	0.191	360.0732	
		130	140	3770.4	0.0254	95.76816	
90	100	110	120	188.52	1.59	299.7468	N5° 32′ 22″ E6° 1′ 11″
		120	130	754.08	0.589	444.1531	
		130	140	1885.2	0.194	365.7288	
100	110	120	130	188.52	2.77	522.2004	N5° 32′ 22″ E6° 1′ 11″
		130	140	754.08	3.44	2594.0352	
110	120	130	140	188.52	1.27	239.4204	N5° 32′ 22″ E6° 1′ 11″

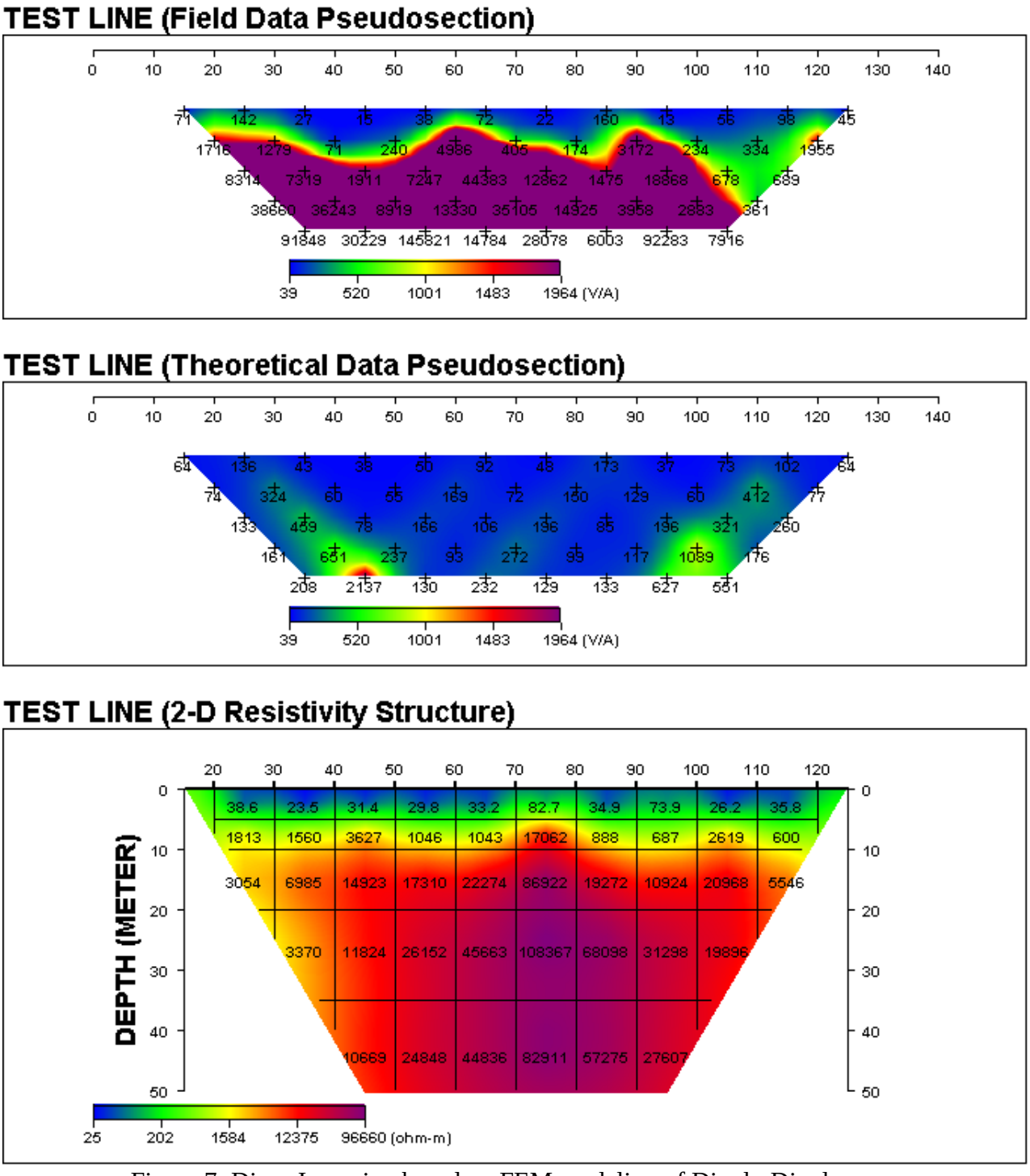

Figure 7: Dipro Inversion based on FEM modeling of Dipole-Dipole array

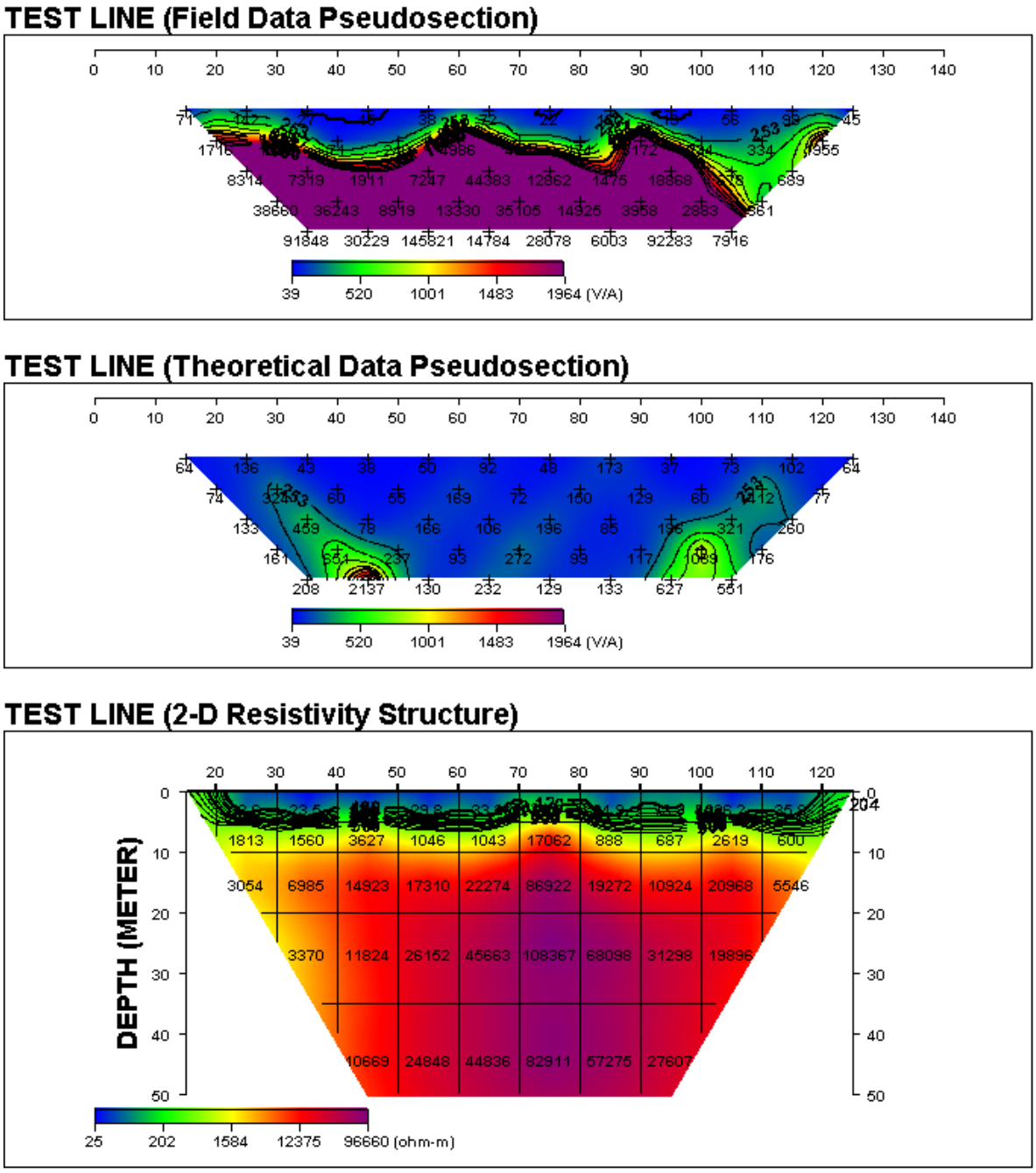

Figure 8: Contour of Dipro Inversion of Dipole-Dipole 2

Table 6: Field data of Dipole-Dipole 2 at Old Dumpsite in Esefieta Layout

RESISTIVITY FIELD RECORD							
Site Description: Old Dumpsite in Esefieta Layout					Operation: Omamode Samuel Marere		
Equipment: Petrozenith Terrameter					Survey direction: SW Direction		
Date :22/08/2024					Electrode Array: Dipole-Dipole 2		
Electrode Spacing: 10m					Elevation:		
Electrode position				Geometric Factor	Resistance Ω	Superficial Resistivity Ωm	Coordinate of Stations
C1	C2	P1	P2				
0	10	20	30	188.52	2.25	424.17	N5˚32′ 22.452″

		30	40	754.08	1.23	927.5184	E6° 1′ 12.936″
		40	50	1885.2	3.12	5881.824	
		50	60	3770.4	1.32	4976.928	
		60	70	6598.2	0.467	3081.3594	
10	20	30	40	188.52	2.16	407.2032	N5° 32′ 21.98″ E6° 1′ 12.654″
		40	50	754.08	0.812	612.31296	
		50	60	1885.2	1.07	2017.164	
		60	70	3770.4	0.119	448.6776	
		70	80	6598.2	0.726	4790.2932	
20	30	40	50	188.52	1.21	228.1092	N5° 32′ 21.732″ E6° 1′ 12.558″
		50	60	754.08	0.593	447.16944	
		60	70	1885.2	1.79	3374.508	
		70	80	3770.4	3.16	11914.464	
		80	90	6598.2	0.373	2461.1286	
30	40	50	60	188.52	1.78	335.5656	N5° 32′ 21.552″ E6° 1′ 12.324″
		60	70	754.08	5.13	3868.4304	
		70	80	1885.2	5.28	9953.856	
		80	90	3770.4	0.958	3612.0432	
		90	100	6598.2	9.76	64398.432	
40	50	60	70	188.52	2.03	382.6956	N5° 32′ 21.168″ E6° 1′ 12.162″
		70	80	754.08	2.4	1809.792	
		80	90	1885.2	0.552	1040.6304	
		90	100	3770.4	0.441	1662.7464	
1		100	110	6598.2	8.83	58262.106	
50	60	70	80	188.52	1.63	307.2876	N5° 32′ 20.886″ E6° 1′ 11.982″
		80	90	754.08	7.5	5655.6	
		90	100	1885.2	8.84	16665.168	
		100	110	3770.4	10.39	39174.456	
60	70	80	90	188.52	1.68	316.7136	N5° 32′ 20.652″ E6° 1′ 12.718″
		90	100	754.08	0.239	180.22512	
		100	110	1885.2	0.0884	166.65168	
70	80	90	100	188.52	2.84	535.3968	N5° 32′ 20.388″ E6° 1′ 11.568″
		100	110	754.08	0.6755	509.38104	
80	90	100	110	188.52	1.17	220.5684	N5° 32′ 20.124″ E6° 1′ 11.399″

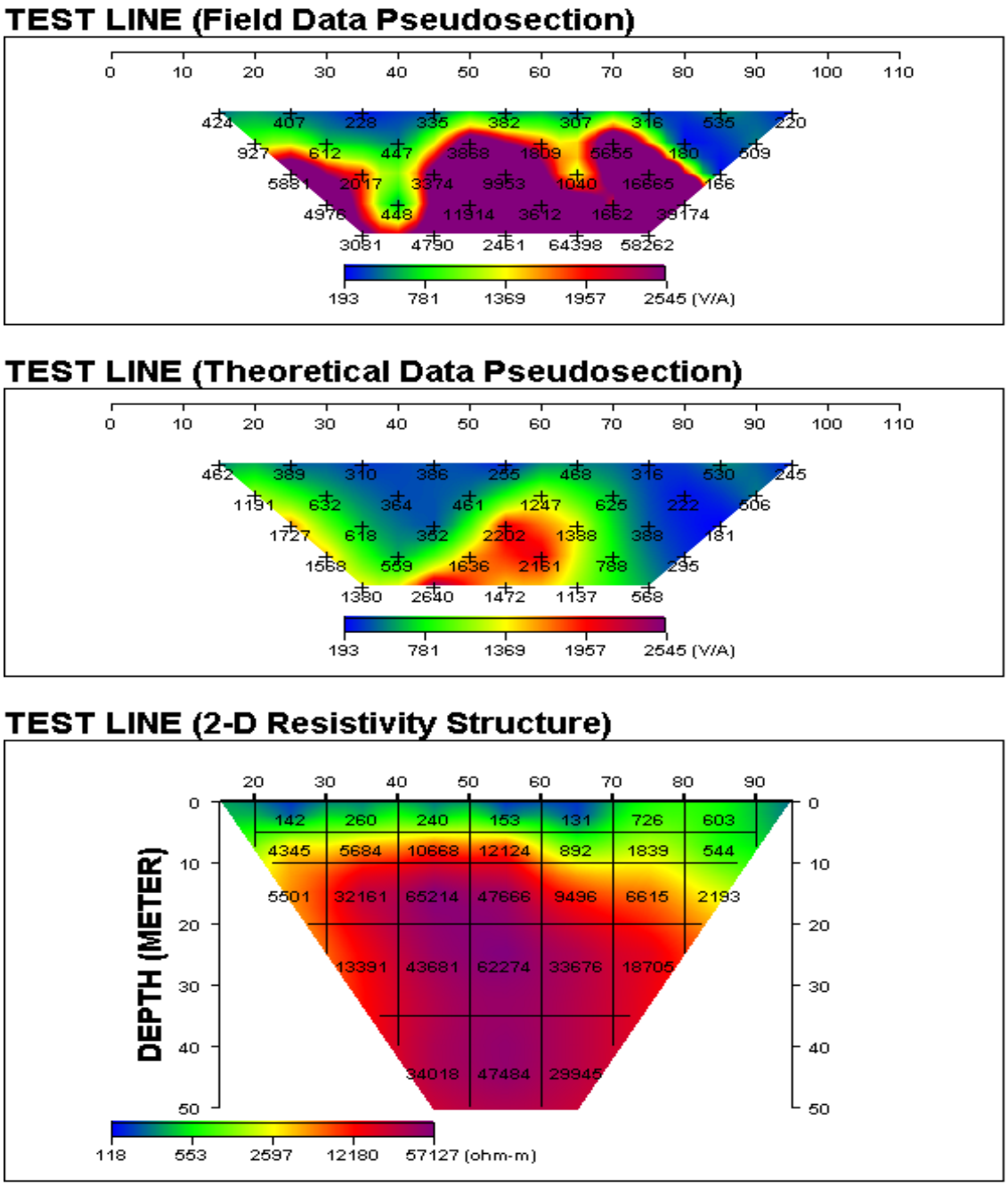

Figure 9: Dipro Inversion based on FEM modeling of Dipole-Dipole 2

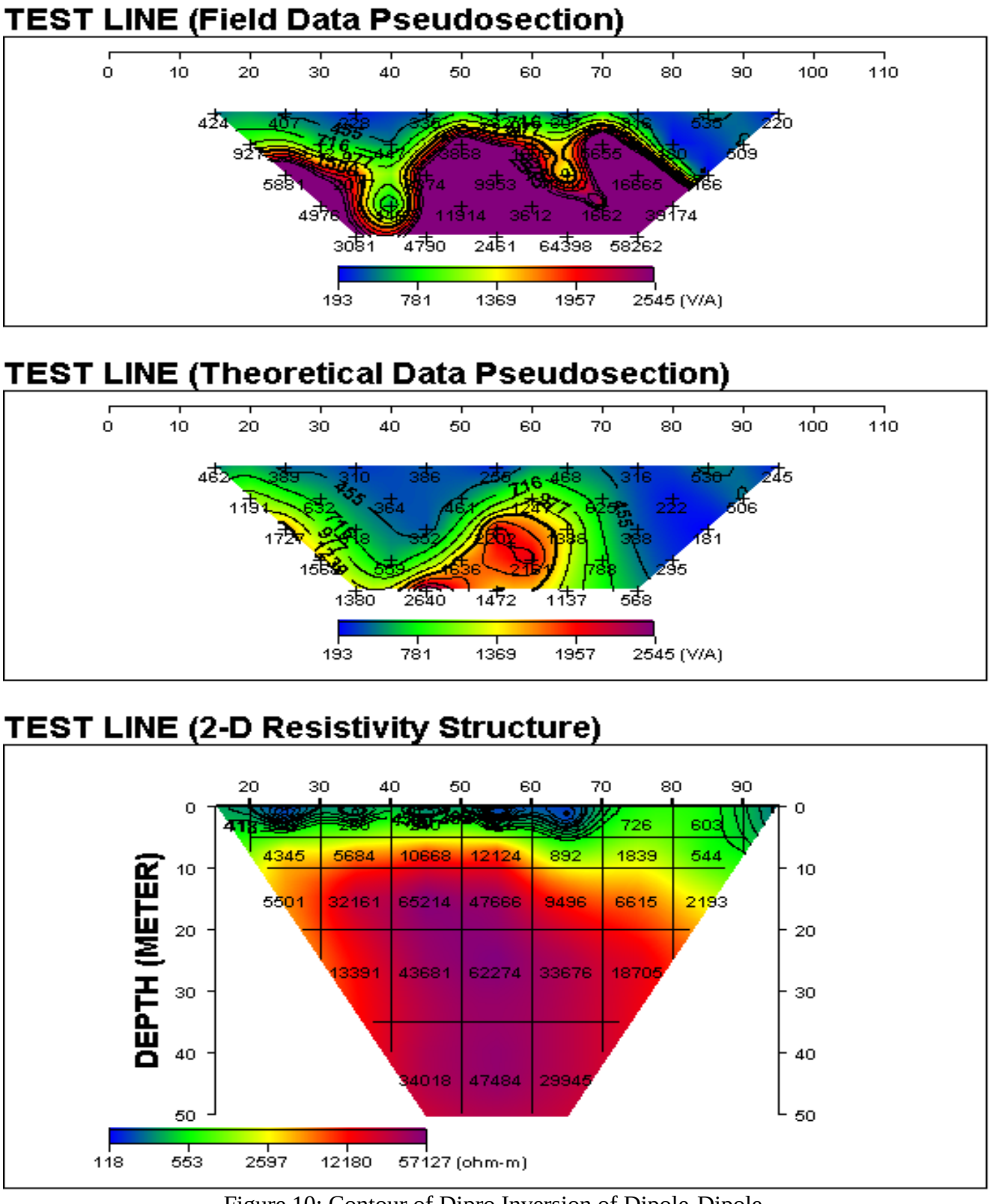

Figure 10: Contour of Dipro Inversion of Dipole-Dipole

Table 7: Field data of Dipole-Dipole 3 along Old Dumpsite in Esefieta Layout express way

RESISTIVITY FIELD RECORD							
Site Description: Old Dumpsite in Esefieta Layout					Operation: Omamode Samuel Marere		
Equipment: Petrozenith Terrameter					Survey Direction: SW		
Date :23/08/2024					Electrode Array: Dipole-Dipole 3		
Electrode Spacing: 10m					Start Point: N5° 32′ 25″ E6° 1′ 9″ End Point: N5° 32′ 21.44″ E6° 1′ 7.05″		
Electrode position				Geometric Factor	Resistance Ω	Superficial Resistivity Ωm	Coordinate point of stations
C1	C2	P1	P2				
0	10	20	30	188.52	20.44	3853.3488	N5° 32′ 25″ E6° 1′ 9″
		30	40	754.08	22.3	16815.984	
		40	50	1885.2	20.25	38175.3	
		50	60	3770.4	7.64	28805.856	
		60	70	6598.2	9.62	63474.684	
10	20	30	40	188.52	18.93	3568.6836	N5° 32′ 25.60″ E6° 1′ 8.98″
		40	50	754.08	12.65	9539.112	
		50	60	1885.2	12.23	23055.996	
		60	70	3770.4	19.62	73975.248	
		70	80	6598.2	11.52	76011.264	
20	30	40	50	188.52	8.95	1687.254	N5° 32′ 25.28″ E6° 1′ 8.83″
		50	60	754.08	18.25	13761.96	
		60	70	1885.2	24.54	46262.808	
		70	80	3770.4	22.4	84456.96	
		80	90	6598.2	17.39	114742.698	
30	40	50	60	188.52	20.98	3955.1496	N5° 32′ 25.06″ E6° 1′ 8.70″
		60	70	754.08	30.17	22750.5936	
		70	80	1885.2	24.14	45508.728	
		80	90	3770.4	15.79	59534.616	
		90	100	6598.2	16.1	106231.02	
40	50	60	70	188.52	8.15	1536.438	N5° 32′ 24.71″ E6° 1′ 8.61″
		70	80	754.08	22.77	17170.4016	
		80	90	1885.2	17.52	33028.704	
		90	100	3770.4	18.48	69676.992	
		100	110	6598.2	8.72	57536.304	
50	60	70	80	188.52	7.07	1332.8364	N5° 32′ 24.11″ E6° 1′ 8.34″
		80	90	754.08	15.04	11341.3632	
		90	100	1885.2	15.73	29654.196	
		100	110	3770.4	15.47	58328.088	
		110	120	6598.2	16.34	107814.588	
60	70	80	90	188.52	9.48	1787.1696	N5° 32′ 23.79″ E6° 1′ 8.20″
		90	100	754.08	13.8	10406.304	
		100	110	1885.2	13	24507.6	
		110	120	3770.4	14.28	53841.312	

		120	130	6598.2	15.32	101084.424	
70	80	90	100	188.52	8.27	1559.0604	N5° 32′ 23.49″ E6° 1′ 8.1″
		100	110	754.08	10.89	8211.9312	
		110	120	1885.2	12.71	23960.892	
		120	130	3770.4	13.31	50184.024	
		130	140	6598.2	12.81	84522.942	
80	90	100	110	188.52	7.97	1502.5044	N5° 32′ 23.29″ E6° 1′ 7.90″
		110	120	754.08	11.37	8573.8896	
		120	130	1885.2	3.24	6108.048	
		130	140	3770.4	5.12	19304.448	
		140	150	6598.2	15.17	100094.694	
90	100	110	120	188.52	9.38	1768.3176	N5° 32′ 23.05″ E6° 1′ 7.75″
		120	130	754.08	12.04	9079.1232	
		130	140	1885.2	11.2	21114.24	
		140	150	3770.4	31.29	117975.816	
100	110	120	130	188.52	9.76	1839.9552	N5° 32′ 22.63″ E6° 1′ 7.64″
		130	140	754.08	11.7	8822.736	
		140	150	1885.2	9.31	17551.212	
110	120	130	140	188.52	8.28	1560.9456	N5° 32′ 22.37″ E6° 1′ 7.5″
		140	150	754.08	13.97	10534.4976	
120	130	140	150	188.52	8.07	1521.3564	N5° 32′ 22.03″ E6° 1′ 7.34″

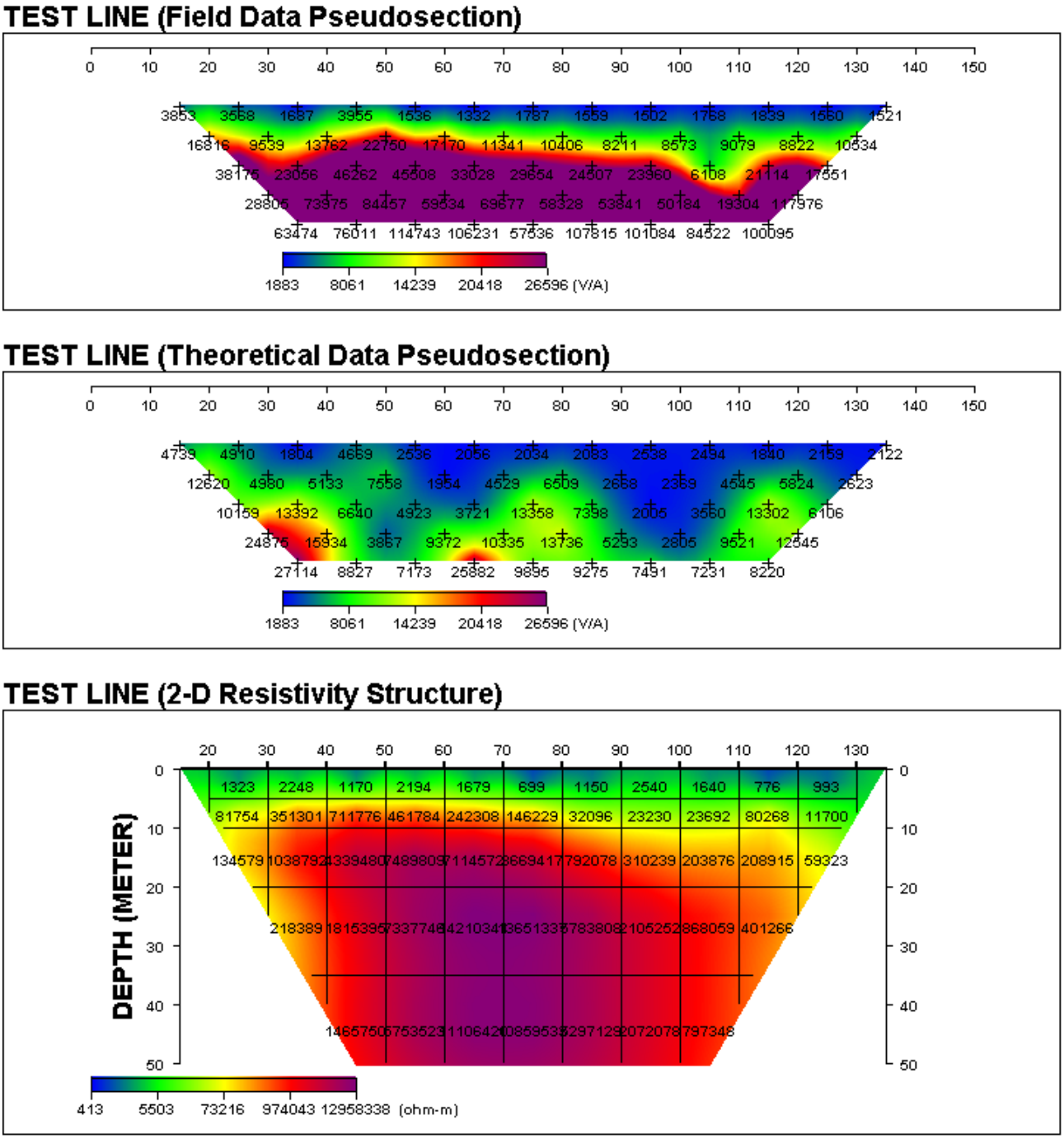

Figure 11: Dipro Inversion based on FEM modeling of Dipole-Dipole 3

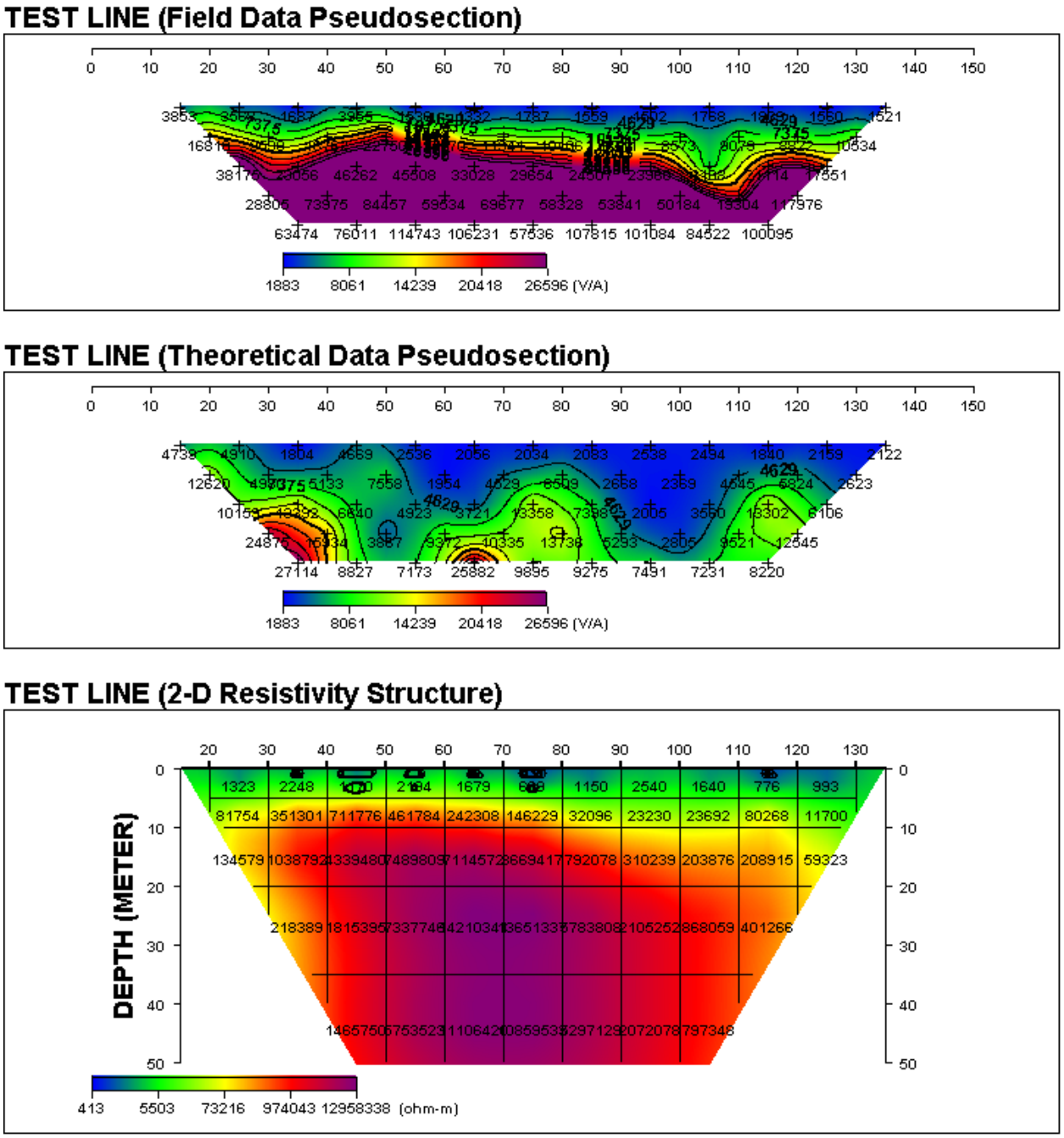

Figure 12: Contour of Dipro Inversion of Dipole-Dipole 3

Table 8: VES 1 Data at Old Dumpsite in Esefieta Layout

VES 1 Data N5° 32′ 24.36″ E6° 1′ 8.424″ N5° 32′ 19.086″ E6° 1′ 15.918″ N5° 31′ 49″ E6° 0′ 52″						
S/N	MN/2 (m)	AB/2 (m)	GEOMETRIC FACTOR	RESISTANCE (Ω)	SUPERFICIAL RESISTIVITY (Ωm)	Lithology
1	0.5	1	4.76	77.76	370.138	Top soil
2	0.5	1.47	10.84	36.3	393.492	Lateritic Soil
3	0.5	2.15	23.7	17.36	411.432	Clay
4	0.5	3.16	51.8	45.12	2337.216	Medium Sand

5	0.5	4.64	112	6.91	773.92	Fine Sand
6	0.5	6.81	242	2.31	559.02	Fine Sand
7	0.5	10	524	1.11	581.64	Fine Sand
8	3	10	47.6	7.74	368.424	Clay
9	3	14.7	108	3.65	394.2	Clay
10	3	21.5	237	1.76	417.12	Clay
11	5	31.6	306	0.9095	278.307	Clay
12	5	46.4	669	0.756	505.764	Fine Sand
13	3	68.1	2424	0.404	979.296	Fine-Medium Sand
14	3	100	5231	0.2168	1134.08	Medium Sand
15	6	100	2609	0.6178	1611.84	Medium Sand
16	6	150	5648	0.1929	1089.499	Medium Sand

Table 9: VES 1 Data with Adjusted Superficial Resistivity and Resistivity Model

VES 1 Data with adjusted Resistivity				Resistivity Model		
S/N	AB/2 (m)	MN/2 (m)	Adjusted Superficial Resistivity (Ωm)	Resistivity (Ωm)	Thickness (m)	Depth (m)
1	1.00	0.5	370.14	308.14	0.7615	0.7615
2	1.47	0.5	423.49	992.19	3.9122	4.6737
3	3.16	0.5	511.43	187.04	8.3617	13.035
4	4.64	0.5	637.22	749.59	5.7960	18.831
5	6.81	0.5	673.92	3906.4	37.960	56.791
6	10.00	0.5	659.02	384.90	Undetermined	Undetermined
7	14.70	3	581.64			
8	21.50	3	504.20			
9	31.60	3	417.12			
10	46.40	3	478.31			
11	68.10	3	635.76			
12	100.00	3	879.30			
13	147.00	6	1034.08			

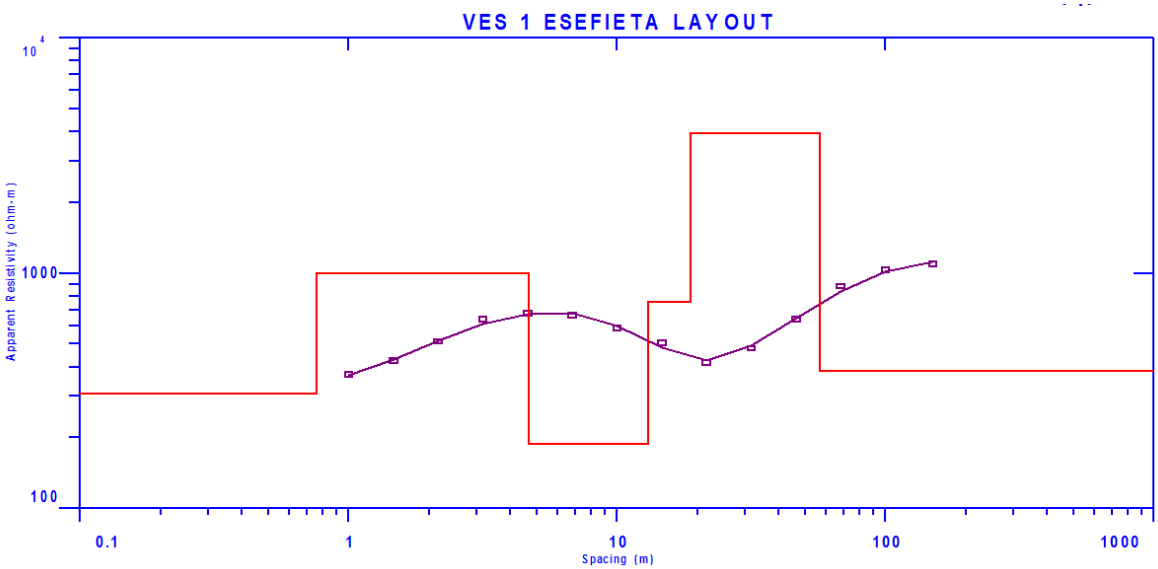

Figure 13: Typical Hydrogeophysical Sounding Curve of VES 1

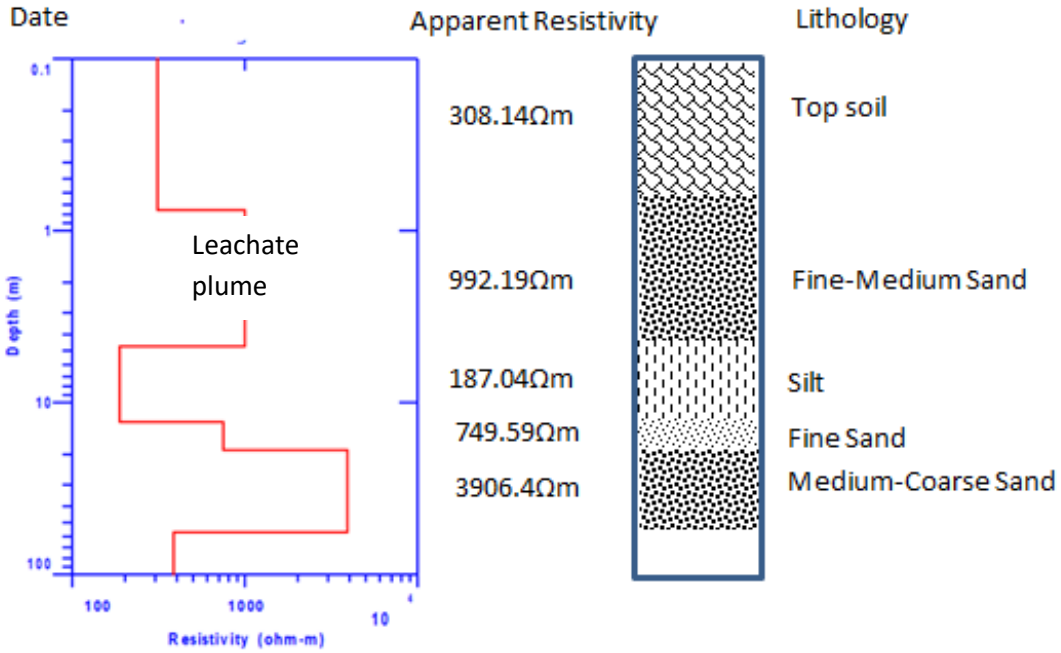

Figure 14: Layered Inversion Model and Lithology of VES 1

Table 10: VES 2 Data with Lithology along Ofuoma Express way off Esefieta Layout

VES 2 Along Ofuoma Express way off Esefieta Layout N5° 32′ 19.33″ E6° 1′ 6.09″ N5° 32′ 23.79″ E6° 1′ 8.26″ N5° 32′ 28.2″ E6° 1′ 10.01″						
S/N	MN/2 (m)	AB/2 (m)	Geometric Factor	Resistance (Ω)	Superficial Resistivity (Ωm)	Lithology
1	0.5	1	4.76	66.1	314.636	Top soil
2	0.5	1.47	10.84	18.71	202.8164	Lateritic soil
3	0.5	3.16	51.8	16.33	845.894	Medium Sand
4	0.5	4.64	112	6.03	675.36	Fine Sand
5	0.5	6.81	242	5.61	1357.62	Medium-Coarse Sand

6	0.5	10	524	3.56	1865.44	Medium-Coarse Sand
7	3	10	47.6	18.3	871.08	Medium Sand
8	3	14.7	108	17.75	1917.0	Medium-Coarse Sand
9	3	21.5	237	6.21	1471.77	Medium-Coarse Sand
10	3	31.6	514	5.18	2662.52	Coarse Sand
11	3	46.4	1123	5.4	6064.2	Very Coarse Sand
12	3	68.1	2424	2.05	4969.2	Very Coarse Sand
13	3	100	2451	1.32	3235.32	Very Coarse Sand
14	6	100	2609	5.39	14062.51	Sandstone
15	6	147	5648	0.41	2315.68	Coarse Sand

Table 11: VES 2 Data with Adjusted Superficial Resistivity and Resistivity Model

VES 2 Data with adjusted Superficial Resistivity				Resistivity Model		
S/N	AB/2 (m)	MN/2 (m)	Adjusted Resistivity (Ωm)	Resistivity (Ωm)	Thickness (m)	Depth (m)
1	1.00	0.5	314.64	125.13	0.3369	0.3369
2	1.47	0.5	382.82	2355.3	15.425	15.762
3	3.16	0.5	845.89	12009	19.101	34.862
4	4.64	0.5	1075.36	845.67	26.091	60.954
5	6.81	0.5	1357.62	279.71	Undetermined	Undetermined
6	10.00	0.5	1865.44			
7	14.70	3	1917.00			
8	21.50	3	2171.77			
9	31.60	3	2662.52			
10	46.40	3	3364.20			
11	68.10	3	3569.20			
12	100.00	3	3235.32			
13	147.00	6	2315.68			

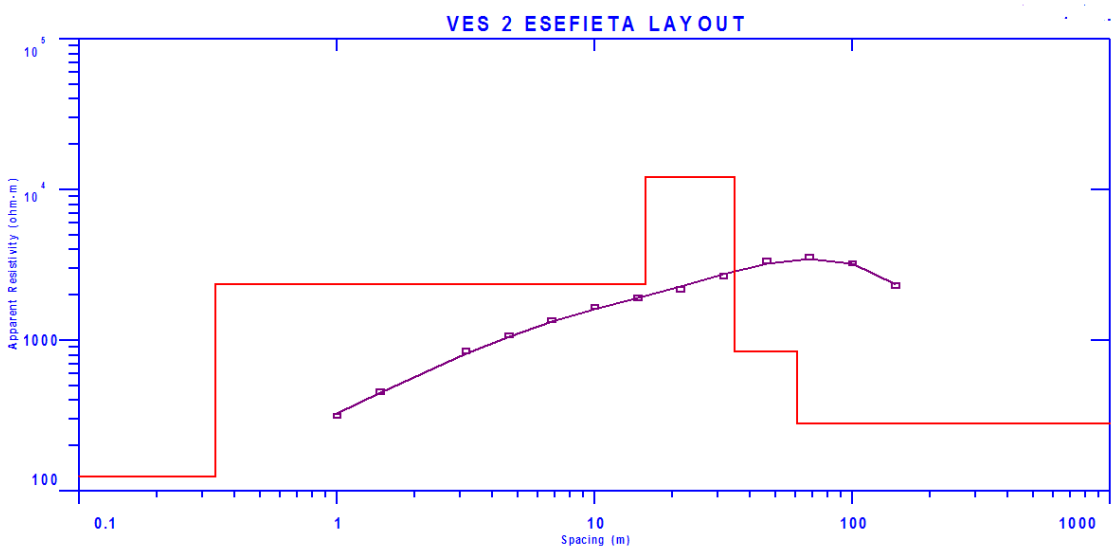

Figure 15: Typical Hydrogeophysical Sounding Curve of VES 2

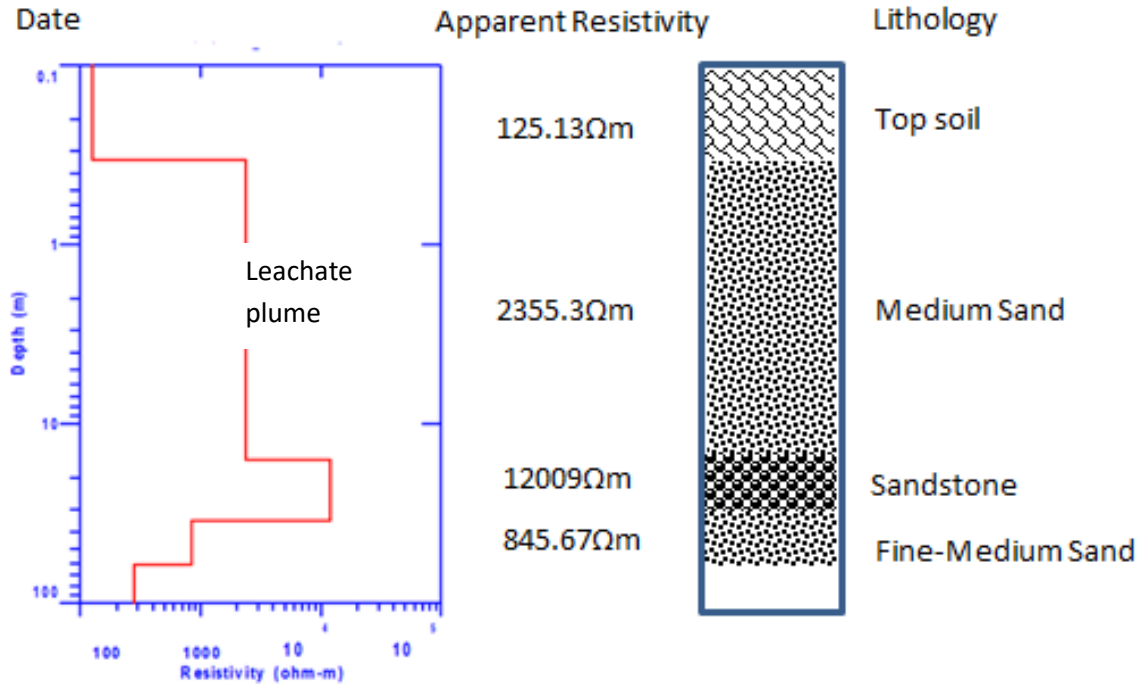

Figure 16: Layered Inversion Model and Lithology of VES 2

4. DISCUSSION

With the exception of pH (4.62), which are above [17] and [18] standard values, the mean concentration of every physiochemical parameter in the water samples examined aligned with the NSDWQ and WHO standard values, as indicated in Table 2 and Figure 2and 3. This suggests that the research area's groundwater is acidic, as the values fall below the neutral pH of 7. Acidic water can cause corrosion of pipes and may pose health risks if consumed over time. The cause could be the discharge from battery electrolytes and other compounds that lower or acidify the water. Figure 2 and 4 shows that loc. 1 has high concentration values of physiochemical parameters followed by loc. 2 and the control is the least. This indicates that water samples collected closer the dumpsite has been impacted by anthropogenic activities.

The concentration value of Magnesium (Mn) ranges from 0.01 to 0.021 mg/L, with an average value of 0.016 mg/L, which conforms to NSDWQ and WHO permissive values of 0.2 mg/L and 50 mg/L. The concentration value of Iron (Fe) ranges from 0.055 to 0.074 mg/L with an average value of 0.0625 mg/L, which conforms to [17] [18], permissive value of 0.3 mg/L. The concentration value of Copper (Cu) ranges from 0.03 to 0.045 mg/L with an average value of 0.038 mg/L, which conform to NSDWQ and WHO permissive values of 1 mg/L and 2 mg/L [17] [18]. The concentration value of Zinc (Zn) ranges from 0.085 to 0.326 mg/L, with an average value of 0.255 mg/L, which conforms to NSDWQ and WHO permissive values of 3 mg/L and 5 mg/L [17] [18]. The concentration value of Cobalt (Co) ranges from 0.009 to 0.013 mg/L, with an average value of 0.007 mg/L, which conforms to NSDWQ and WHO permissive values of 0.05 mg/L and 1 mg/L [17], [18]. The concentration value of Nickel (Ni) ranges from 0.012 to 0.017 mg/L, with an average value of 0.0145 mg/L, which conforms to NSDWQ and WHO permissive values of 0.02 mg/L, [17], [18]. The concentration values of Chromium (Cr) range from 0.012 to 0.016 mg/L, with average value of 0.012 mg/L which conforms to [17] [18] permissive value of 0.05 mg/L as shown in Table 3, Figure 5 and 6.

The concentration of Cadmium (Cd) ranges from 0.01 to 0.17 mg/L, with an average value of 0.0132 mg/L. This is higher than the NSDWQ permissible limit of 0.01 mg/L but remains below the WHO permissible limit of 1 mg/L [18]. Elevated Cadmium levels in the human body can lead to psychological disorders, diarrhea, and immune system damage. The high concentration of Cadmium in the study area may be attributed to the disposal of PVC plastics, cadmium batteries, and metal alloys used for hardening metal parts[19]. The burning of fossil fuels, extraction and melting of metal ores, and the application of phosphate fertilizers are some of the environmental sources of cadmium [20]. The concentration of Lead (Pb) in the study ranges from 0.011 to 0.015 mg/L, with an average of 0.013 mg/L, which exceeds the permissible limit set by [17] [18] of 0.01 mg/L. This contamination is attributed to the industrial nature of the waste disposed around the study area [21]. Consuming water with elevated lead levels can affect red blood cell chemistry, delay normal physical and mental development in infants, and increase blood pressure in adults [21]. Lead is commonly found in tires, plastics, pesticides, coal, automobile batteries. Figures 5 and 6 show that location 1 have the highest concentration of heavy metals, followed by location 2, with the control site having the lowest concentration.

EVALUATION OF THE CONTAMINATION SOURCES OF HEAVY METALS IN WATER SAMPLES USING CORRELATION, HIERARCHICAL CLUSTER ANALYSIS AND PRINCIPAL COMPONENT ANALYSIS.

Out of the forty-five (45) correlation values identified between two parameters, eleven (11) showed an extremely strong positive correlation at the 10% significance level ($P < 0.1$), while seventeen (17) exhibited a strong positive correlation at the 50% significance level ($P < 0.5$). Additionally, five (5) parameters demonstrated an extremely strong negative correlation at the 10% significance level ($P < 0.1$) and this indicates a robust relationship between these parameters, suggesting they are likely influenced by the same factors or sources. While three (3) had a strong negative correlation at the 50% significance level ($P < 0.5$), as illustrated in Table 12. The significant positive correlations between different metal pairs indicate their concurrent release, likely from a common source such as the abandoned dumpsite, as well as their similar transport and accumulation patterns in the water. The importance of these correlations implies that the metals might originate from the same contamination source. Cobalt exhibits very strong and strong negative correlations with other heavy metals. However, Cobalt's negative correlations indicate it likely originates from a different source of pollution origin, as indicated in Table 12.

The dendrogram categorizes the contamination sources of the sampling locations and heavy metals into two distinct clusters, based on their contamination similarity, as indicated in Figures 17 and 18. This clustering helps to identify the groupings of contaminants and locations that share common contamination sources.

The heavy metal values obtained from the water samples were examined using the Principal Component Analysis (PCA) extraction method. This analysis uncovered a single component consisting of interconnected elements and their shared characteristics, as presented in Table 13 [22]. The PCA, detailed in Table 13, revealed a single principal component accounting for approximately 87.356% of the overall variance in the data matrix. This component has an eigenvalue of 7.862, indicating that it explains most of the variance and is likely associated with the primary source of contamination, presumed to be the abandoned dumpsite. The heavy metals associated with Component 1 show a very strong correlation, suggesting they are sourced from a common contamination origin. However, Cobalt (Co) displays a negative correlation with the other metals in this component, implying that it is from a different source of contamination. The scree plot illustrates the relationship between the eigenvalue and the component number. It shows that Component 1 has the highest eigenvalue, indicating its dominance in explaining the variance. Component 2 follows with a lower eigenvalue, while the remaining components (3–9) have minimal eigenvalues and percentages of variance. This highlights that Component 1 is the most significant factor in the dataset, capturing the majority of the variance, as shown in Figure 19.

Table 12: Correlation of heavy metals

	Mn	*Fe*	*Cu*	*Zn*	*Pb*	*Cr*	*Cd*	*Ni*	*Co*
Mn	1								
Fe	0.859412	1							
Cu	0.866818	0.99193	1						
Zn	0.968974	0.924088	0.906506	1					
Pb	0.774213	0.964581	0.981169	0.813599	1				
Cr	0.646208	0.915732	0.879005	0.765581	0.896458	1			
Cd	0.549457	0.831252	0.821812	0.677264	0.804778	0.735543	1		
Ni	0.790967	0.967123	0.980904	0.827179	0.99786	0.908021	0.773192	1	
Co	-0.62287	-0.9351	-0.91488	-0.74739	-0.93399	-0.9553	-0.89454	-0.92645	1

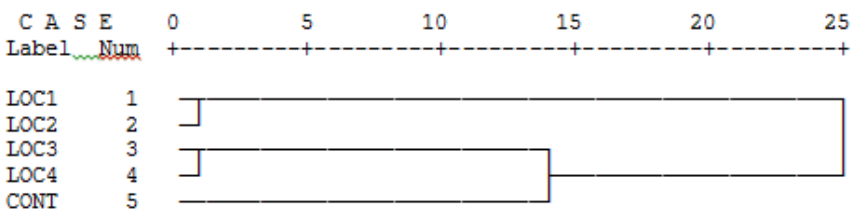

Figure 17: Dendrogram using average linkage to display the contamination relationships between soil groups of different sampling locations.

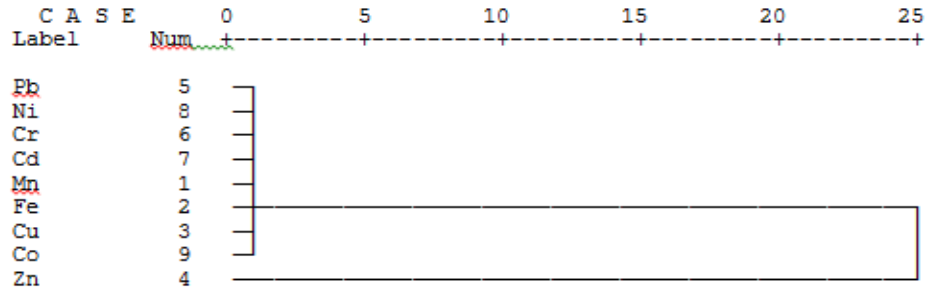

Figure 18: Dendrogram using average linkage to illustrate the contamination relationships between heavy metals.in different soil groups.

Table 13: Summary of PCA (Principal Component Analysis) parameters (Kaiser 1960).

Total Variance Explained						
Component	Initial Eigenvalues			Heavy metals	Component 1	Communalities
	Eigenvalues	% of Variance	Cumulative %	Mn	0.841	0.707
1	7.862	87.356	87.356	Fe	0.999	0.998
2	0.701	7.785	95.141	Cu	0.994	0.987
3	0.288	3.195	98.336	Zn	0.906	0.821
4	0.150	1.664	100.000	Pb	0.974	0.949
Extraction Sums of Squared Loadings				Cr	0.919	0.845
Component	Eigenvalues	% of Variance	Cumulative %	Cd	0.843	0.71
1	7.862	87.356	87.356	Ni	0.975	0.95
				Co	-0.946	0.894

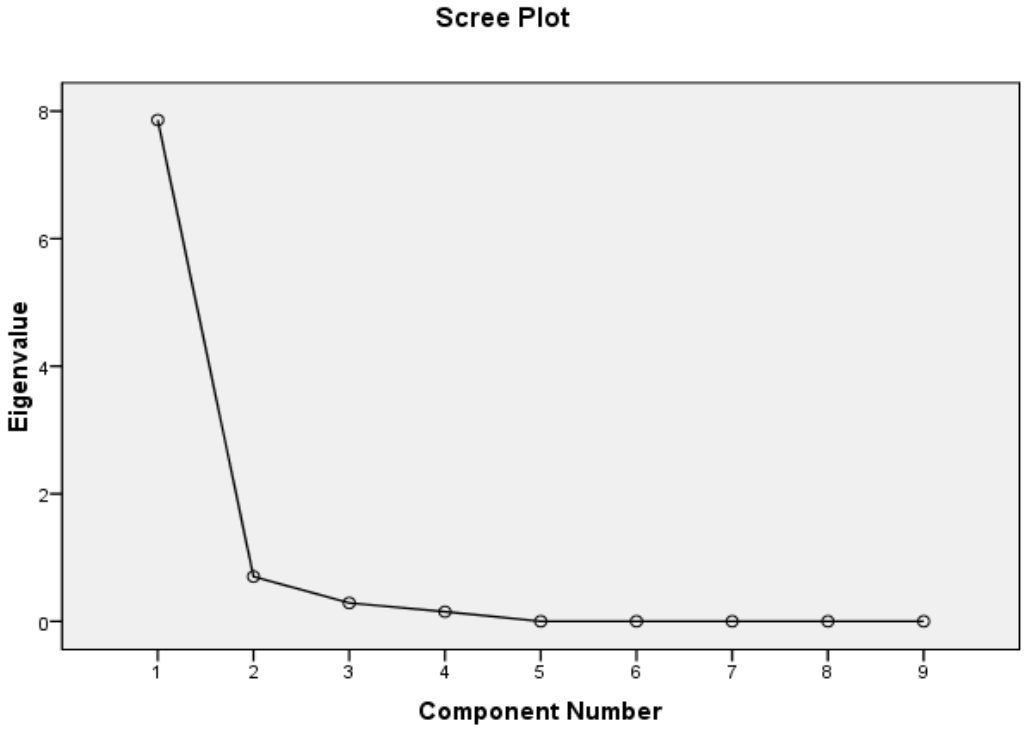

Figure 19: Scree plot showing Eigenvalue against Component number.

SCHLUMBERGER (VES)

From (Table 8, 9 and Figures 13, 14), the resistivity model of VES 1reveals six (6) geoelectric layers. The Apparent resistivity ranges from 308.14Ωm to 3966.4Ωm, overburden has a thickness range from 0.7615 m to 3.9122m and depth ranges from 0.7615m to 4.6737m. The VES reveals that the third geoelectric layer is Silt an average thickness range of 8.3617m at depth range of 13.035m with resistivity range of 187.04Ωm. The fourth and fifth geoelectric layer is fine to coarse Sand with a thickness range from 5.7960m to 37.960m at depth range of 18.831m to 56.791m with resistivity values range from 749.59Ωm to 3966Ωm. The sixth geoelectric layer has an apparent resistivity value of 384.90Ωm with an undetermined thickness and depth. The depth to groundwater ranges from 18.831m to 56.79m with an average depth of 37.81m. The suggested drilling depth to reach groundwater is at 38m (124ft). The curve type is KHA as shown in Figure 13.

From (Table 10, 11 and Figures 15, 16), the VES 2 resistivity model reveals five (5) electrical stratigraphy. The Apparent resistivity spans from 125.13Ωm to 12009Ωm; the overburden layer has a thickness of 0.3369m and depth of 0.3369m. The VES reveals that the third, fourth, fifth geoelectric layer is medium to coarse Sand, Sandstone and fine to medium Sand with a mean thickness range of 15.425m to 26.091m at depth interval of 15.762mto 60.954m with resistivity range of 12009Ωm to 845.67Ωm. The depth to groundwater ranges from 34.86m to 60.98m with an average depth of 47.92m. The advised drilling depth to reach groundwater is at 48m (157ft). The curve type is AAK as shown in Figure 15.

DIPOLE-DIPOLE

From Table 5, Figures 7 and 8), it indicates that the blue coloration signifies leachate with superficial resistivity range of 23.5Ωm to 81.7Ωm, the green coloration signifies the topsoil (surface) of the study area with a superficial resistivity range of 202Ωm to 600Ωm which is composed of clay materials (clay/silt) of low resistivity. The yellow coloration signifies the immediate layer, which has superficial resistivity range of 687Ωm to 1813Ωm which is composed primarily of fine to medium sand, while the light brown coloration denotes the weathered rock with a superficial resistivity range of 3054Ωm to 27607Ωm which is medium to very coarse Sand with little present of gravel and the red coloration indicates bedrock, with a superficial resistivity range of 31298Ωm to 96660Ωm which is primarily composed of Sandstones/basement rock. It is revealed that the leachate has migrated from 20 m to 120 m along the horizontal profiling with a depth range of 0 m to 5m deep. The leachate has deeply penetrated into the soil, contaminating groundwater at 5m depth, due to the high porosity and permeability of the surface soil which facilitates the flow of surface water into the soil.

From Table 6, Figures 9 and 10), it indicates that the blue coloration signifies leachate with a superficial resistivity range of 118Ωm to 142Ωm, the green coloration signifies the topsoil (surface) of the study area, with a superficial resistivity range of 544Ωm to 726Ωm which is primarily composed of fine Sand. The yellow coloration signifies the immediate layer, with a superficial resistivity range of 892Ωm to 2597Ωm which is primarily composed of medium sand, while the light brown coloration represents the weathered rock with a superficial resistivity range of 4345Ωm to 18705Ωm, consisting of very coarse sand with little presence of gravel and the red coloration indicates bedrock, with a superficial resistivity range of 29945Ωm to 57127Ωm which is primarily composed of sandstones/basement rock. The leachate has migrated horizontally from 20m to 40m and 50m to 70m, with a depth of 0m to 5m. It has penetrated deeply into the soil, contaminating the groundwater at a depth of 5m due to the high porosity and permeability of the surface soil, which facilitates the flow of surface water into the soil.

From Table 7, Figures 11 and 12), it indicates that the blue coloration signifies leachate with a superficial resistivity range of 413Ωm to 776Ωm. The green coloration signifies the topsoil (surface) of the study area

with a superficial resistivity range of 1170Ωm to 11700Ωm which is primarily composed of medium to coarse Sand. The yellow coloration signifies the immediate layer, with a superficial resistivity range of 59323Ωm to 81754Ωm which is primarily composed of very coarse sand with the presence gravels. The light brown coloration represents the weathered rock, with a superficial resistivity range of 146222Ωm to 974048Ωm which is sandstone and the red coloration signifies bedrock, with a superficial resistivity range of 16792098Ωm to 12958338Ωm which is primarily composed of basement rock. The leachate has migrated horizontally from 70m to 80m and 110m to 130m, within a depth range of 0m to 5m. it has penetrated deeply into the soil, contaminating the groundwater at a depth of 5m due to high porosity which allows the surface water to flow into the soil,

CONCLUSION

The analysis of water samples from the study area reveals that the majority of the physicochemical parameters meet the standards set by NSDWQ (2007) and WHO (2011). However, the groundwater's pH levels are below these standards, indicating acidity, which could increase the solubility and mobility of metals, thereby raising potential health risks. Although the concentrations of most heavy metals fall within acceptable limits, Lead (Pb) and Cadmium (Cd) exceed permissible levels. **Lead (Pb)** poses serious health risks, particularly by disrupting red blood cell chemistry and raising blood pressure in adults. Its presence in groundwater is often associated with industrial waste, batteries, or fuel sources. **Cadmium (Cd)**, at elevated levels, can lead to psychological disorders, gastrointestinal issues, and immune system damage, commonly originating from industrial activities like metal refining, battery production, and plastics. The analysis suggests that most heavy metals have a common source and follow similar transport pathways in the water, likely linked to pollution from an abandoned dumpsite or industrial activities. However, **Cobalt (Co)** shows a distinct pattern, indicating it may originate from a different or localized source of pollution. Given these findings, while most water quality parameters are within regulatory limits, the acidic groundwater combined with elevated Pb and Cd levels poses significant health risks. The unique behaviour of Co suggests multiple sources of contamination affecting the water quality in the area. Geochemical analysis shows higher contaminant concentrations in wells located closer to the dumpsite, indicating leachates have entered the aquifer system.

To address the water's acidity, it is recommended to install calcite neutralizer filters in the boreholes. These filters gradually dissolve calcite (calcium carbonate) to raise the pH, making the water safer for consumption and reducing health risks associated with acidic groundwater.

The geophysical survey identifies low-resistivity zones beneath the dumpsite, indicating leachate infiltration into the subsurface. The leachate plume from the dumpsite has reached depths of 5m (16ft) to 10m (33ft), potentially contaminating all hand-dug wells in the study area, rendering them unsuitable for consumption. The area's geology consists of clay and fine to very coarse sand, with a recommended drilling depth to groundwater of about 32m (150ft). The shape of the curve from the Vertical Electrical Sounding (VES) data verifies that the study area is of sedimentary composition. The combined geophysical and geochemical approach confirms aquifer contamination beneath the abandoned dumpsite in Ogbovwan Town. The findings emphasize the need for remediation strategies, such as waste removal, soil stabilization, and aquifer treatment, to protect groundwater quality in the region. Furthermore, implementing effective waste management practices is crucial to prevent future environmental hazards.

ACKNOWLEDGEMENTS

This research was made possible by Institution Based Research (IBR) grant sponsored by Nigeria’s Tertiary Education Trust Fund (TETFund).

REFERENCES

[1] Durible JO, Ogwuegbu MOC, Egwurugwu JN. 2007. Pollution profiles of non-metallic inorganic and

organic pollutants of drinking and potable waters due to mining activities in Ishiogu, Ebonyi State, Nigeria. International Journal of Physical Science. 2, 2007,234-238.

[2] Bolaji TA, Tse CA. Spatial variation in groundwater geochemistry and water quality index in Port-Harcourt. Scientia Africana. 8(1), 2009,134-155.

[3] Noel MR, Benson RC, Glaccum RA. The use of contemporary geophysical techniques to aid design of cost-effective monitoring well networks and data analysis. In: Proceedings of second national symposium on aquifer restoration and ground water monitoring, Columbus, Ohio, 1982, pp. 163-168.

[4] Andre-Obayanju O, Aladin AE, Okoroafor, EE. Evaluation of Water Quality within and around Flood Prone area and Dumpsite Environment in Part of Benin Metropolitan city Southern, Nigeria. Pollution and Effects on Community Health, 2023, pp. 1-12.

[5] Madu AN, Agbasi UM, Uzoma EI. Physico-Chemical and Heavy Metal Profiles of Marine, Borehole and Sea Water in Badagry, Lagos State, Nigeria. International Journal of Scientific Research in Chemistry (IJSRCH). 3(2), 2018,19-27.

[6] Ikhile C. Geomorphology and Hydrology of the Benin Region, Edo State, Nigeria. International Journal of Geoscience. 7, 2016,144-157.

[7] Chambers, JE, Kuras O, Meldrum PI, Ogilvy RD, Hollands J. Electrical resistivity tomography applied to geological, hydrogeological and engineering investigations at a former waste disposal site. Geophysics, 71, 2006, B231-B239.

[8] Nwankwoala OH, Amachree T. The water quality index (WQI) and hydrochemical characterization of groundwater resources in hydrocarbon polluted sites in the Niger Delta. Journal of Mining and Geology. 56(1), 2020,69-84.

[9] Olawuyi AK, Abolarin SB. Evaluation of Vertical Electrical Sounding Method for Groundwater Development in Basement Complex Terrain of West-Central Nigeria. Nigeria Journal of Technological Development. 10(2), 2006,22-28.

[10] Anomoharan O. 2013. Geophysical Investigation of Groundwater Potential in Ukelegbe. Nigeria Journal of Applied Sciences. 13, 2013,119-125.

[11] Rai SN. Aquifer Mapping and Sustainable Development. American Society of Civil Engineering. 7, 2017,217-232.

[12] Aladin AE, Sikiru S, Omasan A. Determination of Groundwater Status and Characteristics of the Subsurface Layers Using Electrical Vertical Sounding (VES) and Dipole-Dipole Configuration at Osasogie Road and Environs Southern, Nigeria. International Journal of Earth Sciences Knowledge and Application. 5(2), 2023,282-292.

[13] Alile OM, Aigbogun CO, Abrahim EM, Ighodalo, JE. 2017. 2D and 3D electrical resistivity tomography (ERT) investigation of mineral deposits in Amahor, Edo State, Nigeria. Nigeria Research Journal of Engineering and Environmental Sciences. 2(1), 2017,215-231.

[14] Cyril CO. Sensitivity and Resolution Capacity of Electrode Configurations. Hindawi Publishing Corporation. International Journal of Geophysics. 1, 2013,1-12.

[15] Loke, M.H. Tutorial for 2-D and 3-D electrical imaging surveys, 2004, pp. 1-67.

[16] Aladin AE, Ogueh DE. Influence of Selected Soil Properties on Groundwater Flow around Ariaria Dumpsite, Aba, Southeast, Nigeria. Journal of Applied Sciences and Environmental Management. 28(3), 2024,649-658.

[17] NSDWQ. Nigerian Standard for Drinking Water Quality. Nigerian

Industrial Standard. NIS 554: 2007 ICS 13.060.20, 2007.

[18] WHO. Guidelines for drinking water quality. 4th Edition World Health Organization, Geneva, Switzerland. 2011.

[19] Aladin SE, Ekewenu EE, Osisanya OW. A Comprehensive Analysis of soil and water contamination near auto-mechanic workshops in Warri and Environ South-South, Nigeria. Earth Science Malaysia ESMY. 8(1), 2024,7-20.

[20] Challa S, Kumar R. (2009). Nanostructure oxides. Weinheim, Germany, Wiley, 2009. pp. 29.

[21] Aladin A.E, Omoruyi DI, Odia-Oseghale JO. Impact of Heavy Metals on the Soil and Groundwater of Ariaria Waste Dumpsite, Aba, South-Eastern Nigeria. International Journal of Earth Sciences Knowledge and Application. 4(3), 2022,365-374.

[22] Kaiser HF. The application of electronic computer to factor analysis. Educational and Psychological Measurement, 20, 1960,141-151